Supplementary Information

Inhibition of mechanical allodynia in neuropathic pain by TLR5-mediated A-fiber blockade

Zhen-Zhong Xu, Yong-Ho Kim, Sangsu Bang, Yi Zhang, Temugin Berta, Fan Wang, Seog-Bae Oh, & Ru-Rong Ji

Supplementary Table: 1

Supplemental Figures: 12

Supplementary Table 1. Mouse sequences of *Tlr* primers used for quantitative RT-PCR.

List of primer sequences designed for quantitative real-time RT-PCR.

	Forward primers	Reverse primers	Accession No.
Gapdh	TTGATGGCAACAATCTCCAC	CGTCCCGTAGACAAAATGGT	NM_001001303
Tlr1	ATGTGAGCTGAGGGACTTTG	GGATAGTGGAGACATGTGGAAG	NM_030682
Tlr2	ACCAAGATCCAGAAGAGCCA	CATCACCGGTCAGAAAACAA	NM_011905
Tlr3	GCGTTGCGAAGTGAAGAACT	TTCAAGAGGAGGGCGAATAA	NM_126166
Tlr4	TTCAGAACTTCAGTGGCTGG	TGTTAGTCCAGAGAAACTTCCTG	NM_021297
Tlr5	GCAGGATCATGGCATGTCAAC	ATCTGGGTGAGGTTACAGCCT	NM_016928
Tlr6	CCAAGAACAAAAGCCCTGAG	TGTTTTGCAACCGATTGTGT	NM_011604
Tlr7	GATGTCCTTGGCTCCCTTC	TTTGTCTCTTCCGTGTCCAC	NM_133211
Tlr8	CGTTTTACCTTCCTTTGTCTATAGAAC	CGTCACAAGGATAGCTTCTGG	NM_133212
Tlr9	AACCGCCACTTCTATAACCAG	GTAAGACAGAGCAAGGCAGG	NM_031178
Tlr11	CAGGCTGGGATTGCTCATC	CCAGTCAAGGTAAGGCTCAC	NM_205819
Tlr12	GCTCTGATTCCTCTGGTGTAG	AGAATGTGAAATAGCGGGAGAC	NM_205823
Tlr13	GGAGCGCCTTGATCTAACTAACA	TCAGGTGGGTCAGAGAAACCA	NM_205820

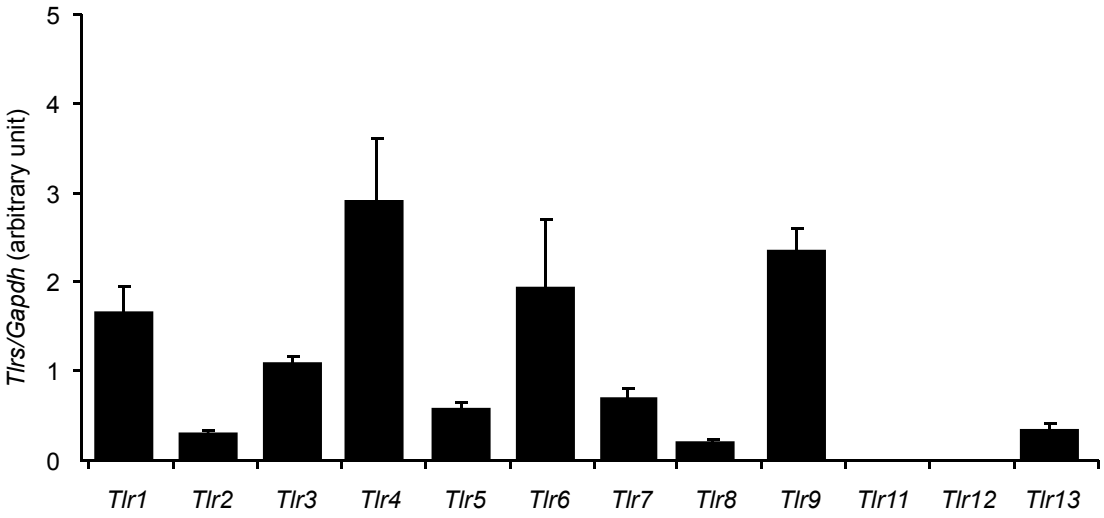

Supplementary Fig. 1. Quantitative RT-PCR analysis shows relative expression of *Tlr mRNA*s in mouse DRG tissues. The values are normalized to GAPDH. n = 3-4 mice/group. All data were expressed as mean ± s.e.m

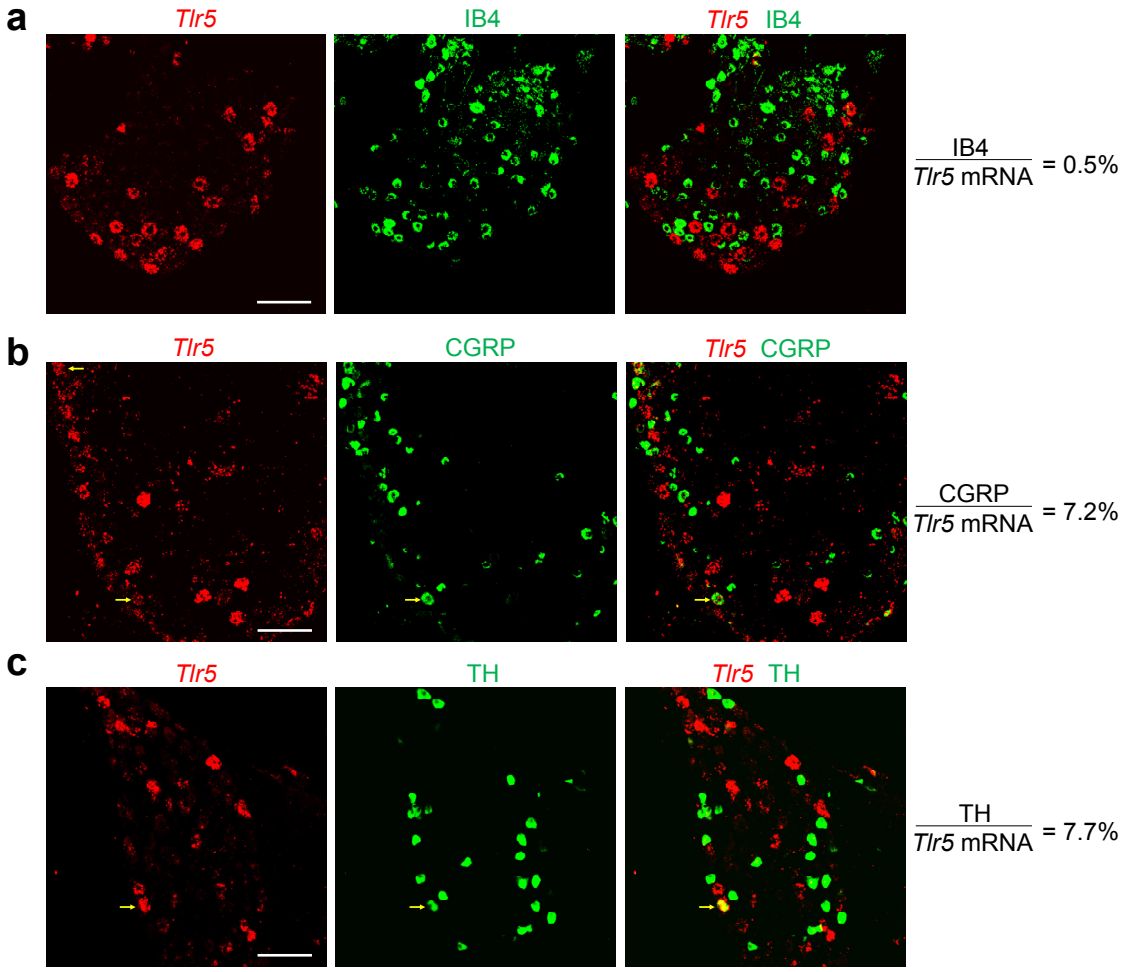

Supplementary Fig. 2. Co-expression of *Tlr5* mRNA with IB4 (**a**), CGRP (**b**), and TH (**c**) in mouse DRG neurons. *Tlr5* mRNA expression was revealed by in situ hybridization. Within the *Tlr5* population, 7.2% of DRG neurons express CGRP and 7.7% of DRG neurons express tyrosine hydroxylase (TH), but only 0.5% of DRG neurons bind IB4. Scale, 100 μm. 4-5 DRG sections per mouse and 3 mice per group were used for percentage quantification.

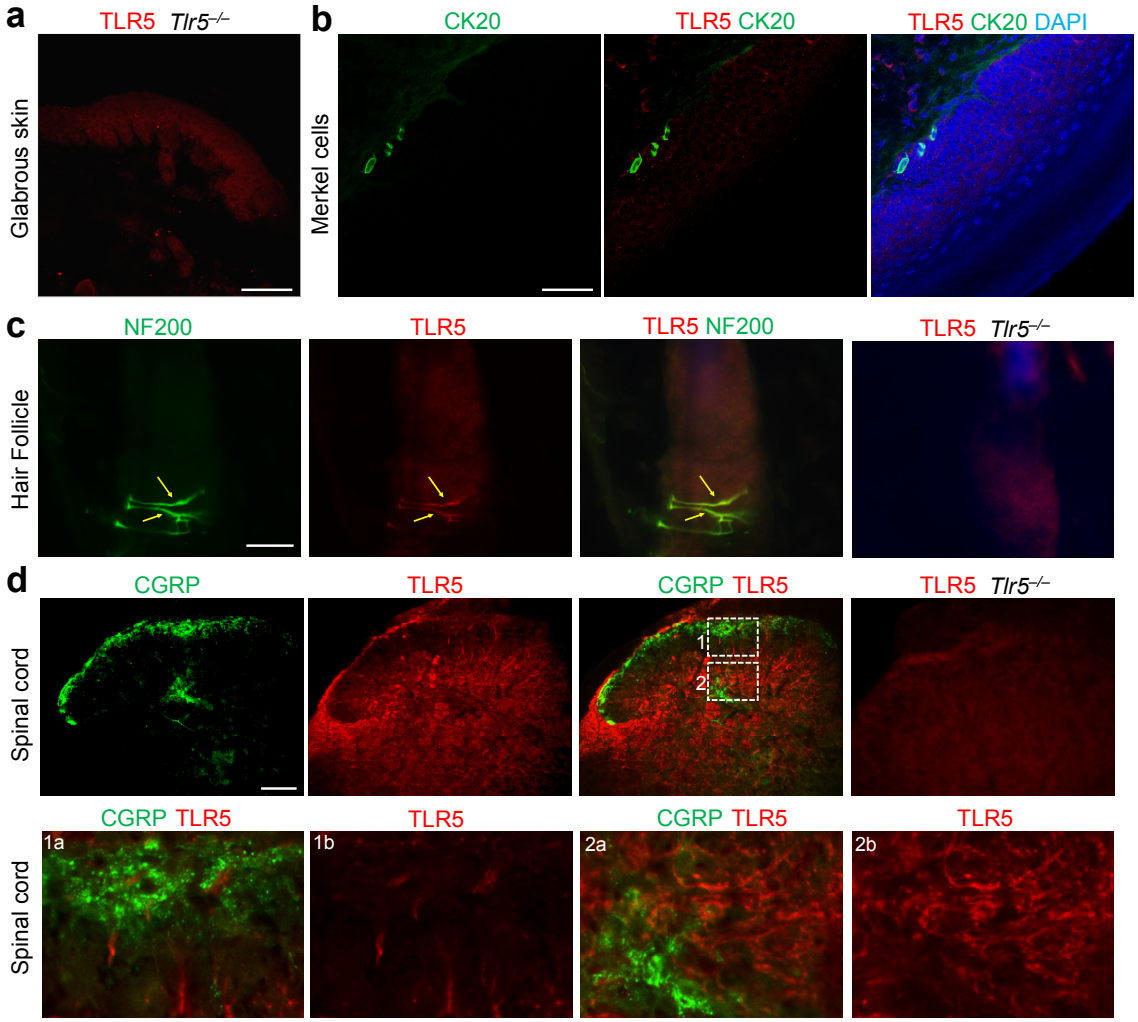

Supplementary Fig. 3. TLR5 expression in skin and spinal cord of WT and *Tlr5*$^{-/-}$ mice. (**a**) TLR5 immunostaining is absent in glabrous skin of *Tlr5*$^{-/-}$ mice. (**b**) Double staining of TLR5 and CK20, a marker for Merkel cells, in hindpaw skin. Note there is no TLR5 staining around Merkel cells. Scale, 100 μm. The skin morphology was revealed by DAPI nuclear staining. (**c**) Double staining of TLR5 and NF200 in hairy skin of WT and *Tlr5*$^{-/-}$ mice. TLR5-IR is present in nerve fibers surrounding the base of hair follicle. Yellow arrows indicate double-labeled nerve fibers. TLR5 staining is absent in *Tlr5*$^{-/-}$ mice. Scale, 20 μm. (**d**) Double immunostaining of TLR5 and CGRP in spinal cord dorsal horn. Box-1 and Box-2 in the dorsal horn are enlarged in low panels. 1a and 2a are merged images, and 1b and 2b are TLR5 single staining images. Note there is no obvious co-localization of TLR5 and CGRP in spinal cord axons and axonal terminals. Scale, 100 μm.

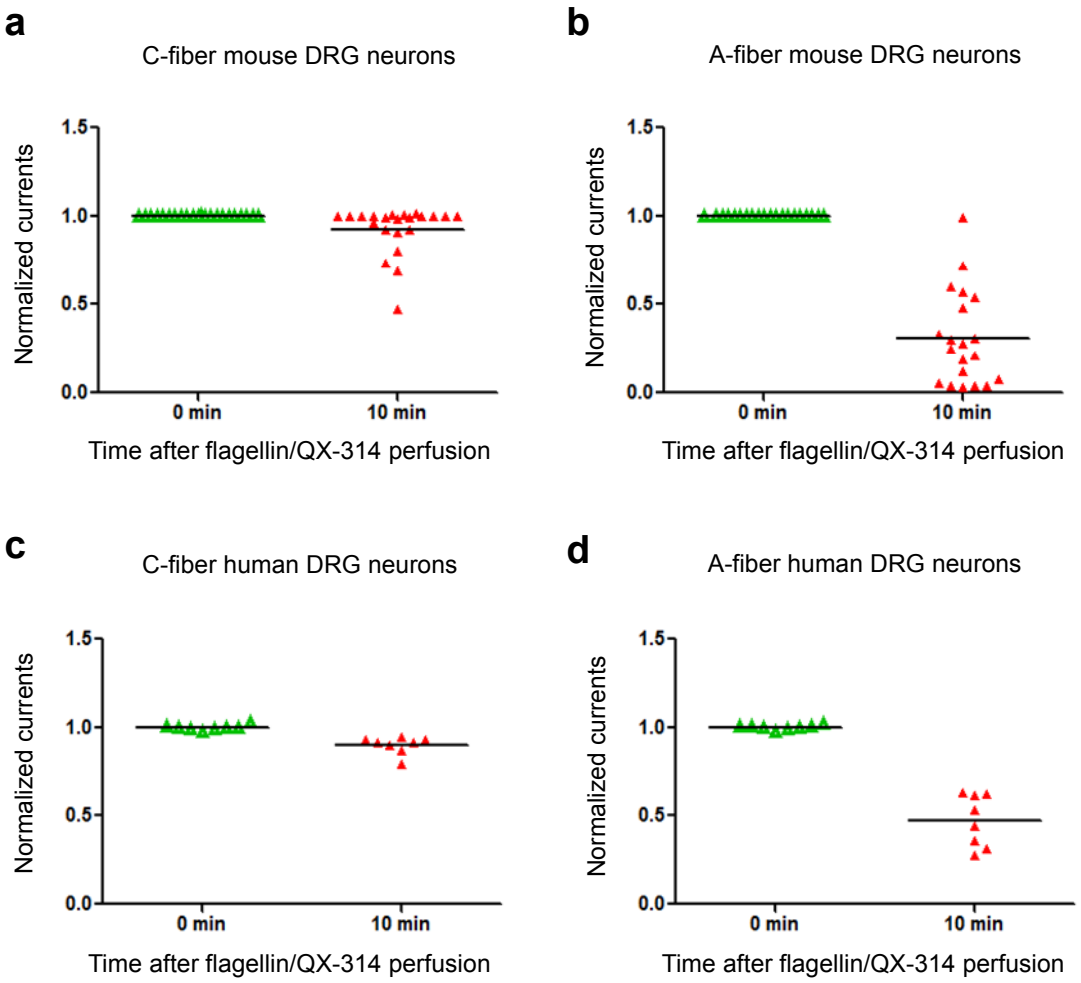

Supplementary Fig. 4. Summary of mouse and human DRG neurons' responses to A-fiber blockade. (**a**) C-fiber and (**b**) A-fiber DRG neurons' responses to A-fiber blockade (0.3 nM flagellin and 5 mM QX-314) in mice. n = 22 neurons for C-fibers and n = 20 neurons for A-fibers. Y-axis shows normalized sodium currents (amplitude, normalized to the baseline) at 0 min and 10 min after QX-314/flagellin treatment. Note a marked reduction in currents in A-fiber neurons (30-55 μm). A few C-fiber (10-25 μm) neurons also display moderate inhibition. (**c**) C-fiber and (**d**) A-fiber human DRG neurons' responses to A-fiber blockade (0.9 nM flagellin and 12 mM QX-314). n = 8 neurons per group.

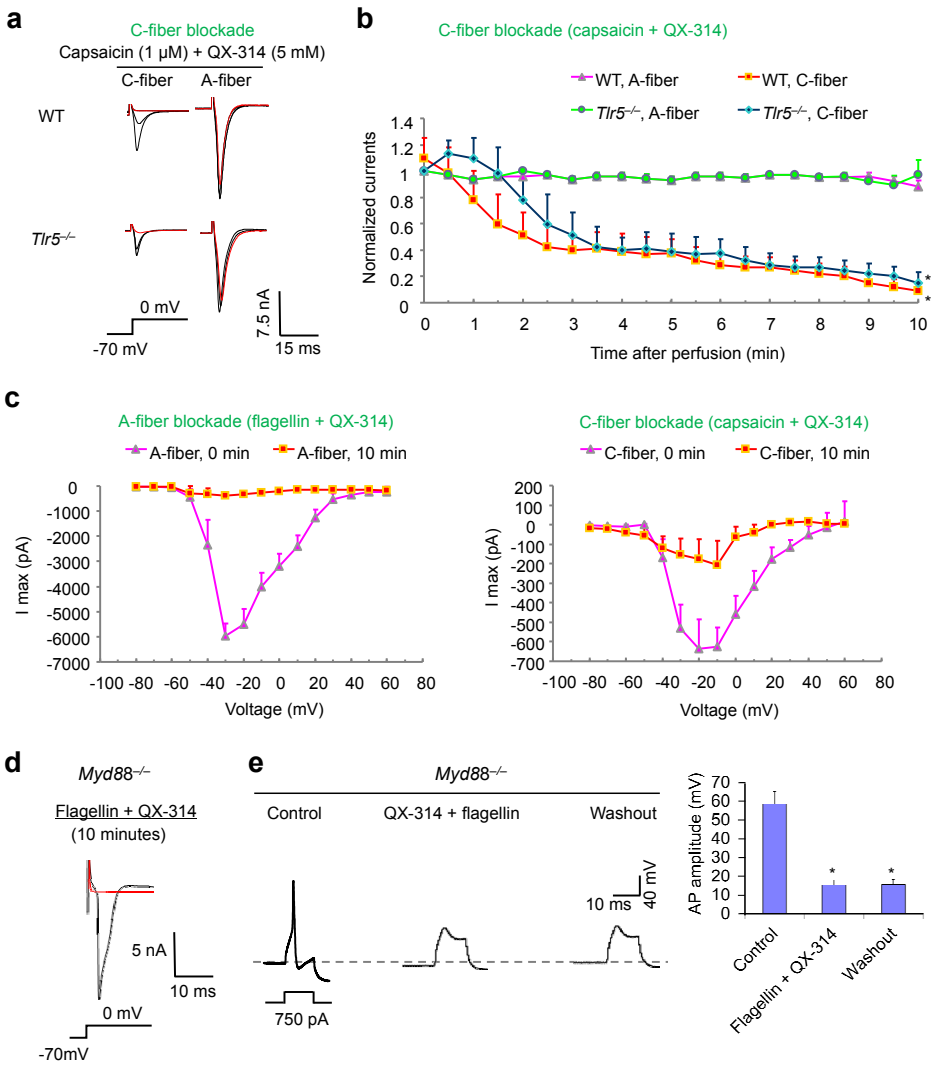

Supplementary Fig. 5. Effects of C-fiber blockade on sodium currents in small C-fiber and large A-fiber DRG neurons in WT and *Tlr5*$^{-/-}$ mice and effects of A-fiber blockade in *Myd88*$^{-/-}$ mice. (**a**) Traces of transient sodium currents in C- and A-fiber neurons of WT and *Tlr5*$^{-/-}$ mice, before and after C-fiber blockade (1 μM capsaicin / 5 mM QX-314). (**b**) Time course of sodium currents in C- and A-fiber neurons after C-fiber blockade. C-fiber blockade via capsaicin/QX-314 suppresses sodium currents and action potentials in small C-fiber but not large A-fiber DRG neurons. Note that the effect of C-fiber blockade is not affected in *Tlr5*-deficient neurons. **P* < 0.05, two-way ANOVA. *n* = 10 neurons/group. (**c**) I/V curves of A-fiber blockade and C-fiber blockade. (**d**) Traces of transient sodium currents in A-fiber neurons of *Myd88*$^{-/-}$ mice before and after flagellin/QX-314 (A-fiber blockade). (**e**) Traces of action potentials in A-fiber neurons of *Myd88*$^{-/-}$ mice before and during flagellin/QX-314 treatment and after washout. Right, amplitude of action potentials. Note that A-fiber blockade retains its efficacy in *Myd88*$^{-/-}$ mice. **P*<0.05, vs. control, *n* = 10 neurons/group. All data were expressed as mean ± s.e.m.

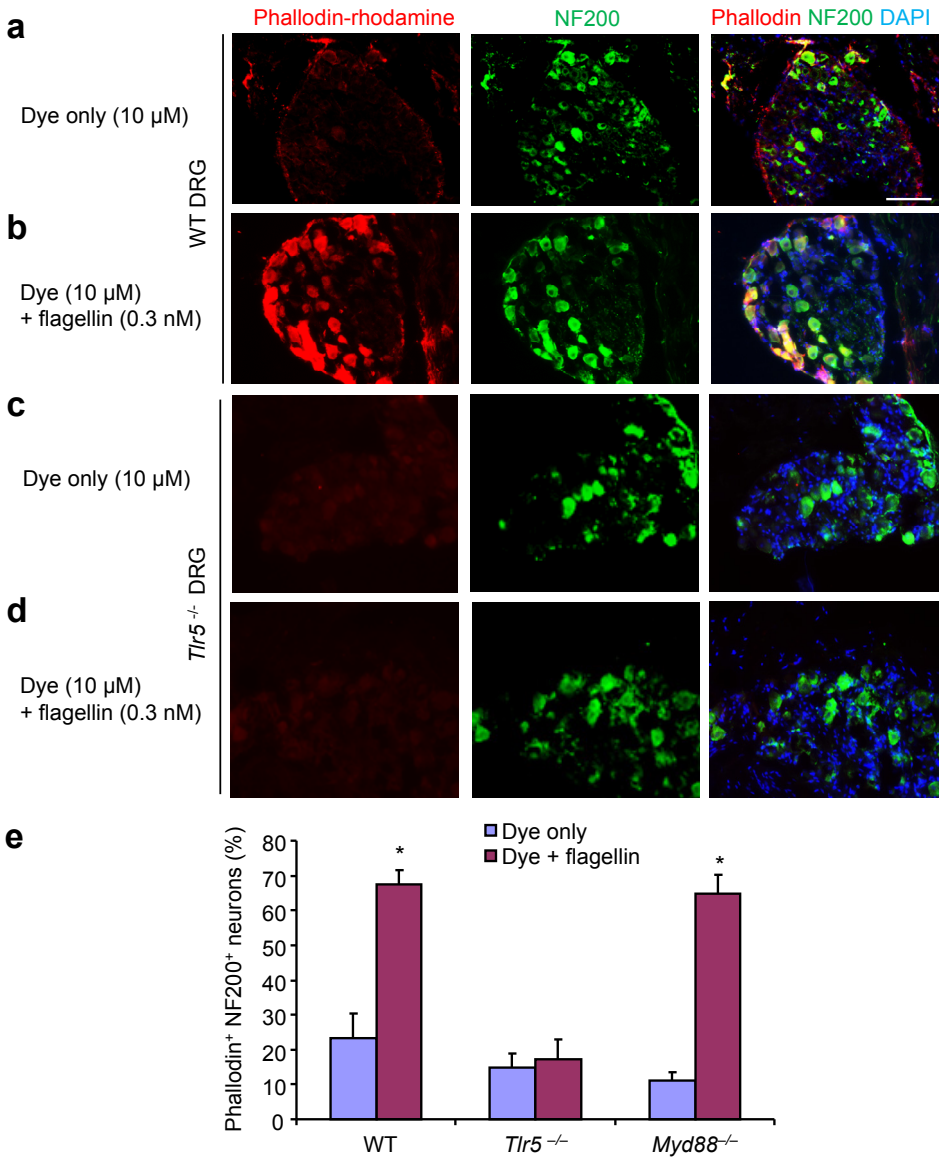

Supplementary Fig. 6. Flagellin/QX-314 treatment causes entry of phallodin-rhodamine into large A-fiber DRG neurons via TLR5 activation. (**a-d**) Double labeling of phallodin-rhodamine (red) and NF200 (green) in DRG sections of WT mice (**a,b**) and *Tlr5*$^{-/-}$ mice (**c,d**) after treatment of flagellin (**a,c**) and flagellin/QX-314 (**b,d**). Whole mount DRGs were treated with 0.3 nM flagellin or 0.3 nM flagellin / 5 mM QX-314 for 10 min. After the treatment, the DRGs were fixed and processed for NF200 immunostaining and DAPI DNA staining (blue). Note that only flagellin/QX-314 co-application induces phallodin entry into NF200-expressing neurons in WT but not *Tlr5*$^{-/-}$ mice. Scale, 100 μm. (**e**) Percentage of phallodin-rhodamine/NF200 double-labeled neurons following dye incubation with and without flagellin/QX-314 in WT, *Tlr5*$^{-/-}$ mice, and *Myd88*$^{-/-}$ mice. Note that phallodin-rhodamine entry is blocked after *Tlr5* but not *Myd88* deficiency. *$P <$ 0.05, $n = 3$ mice/group. All data were expressed as mean ± s.e.m.

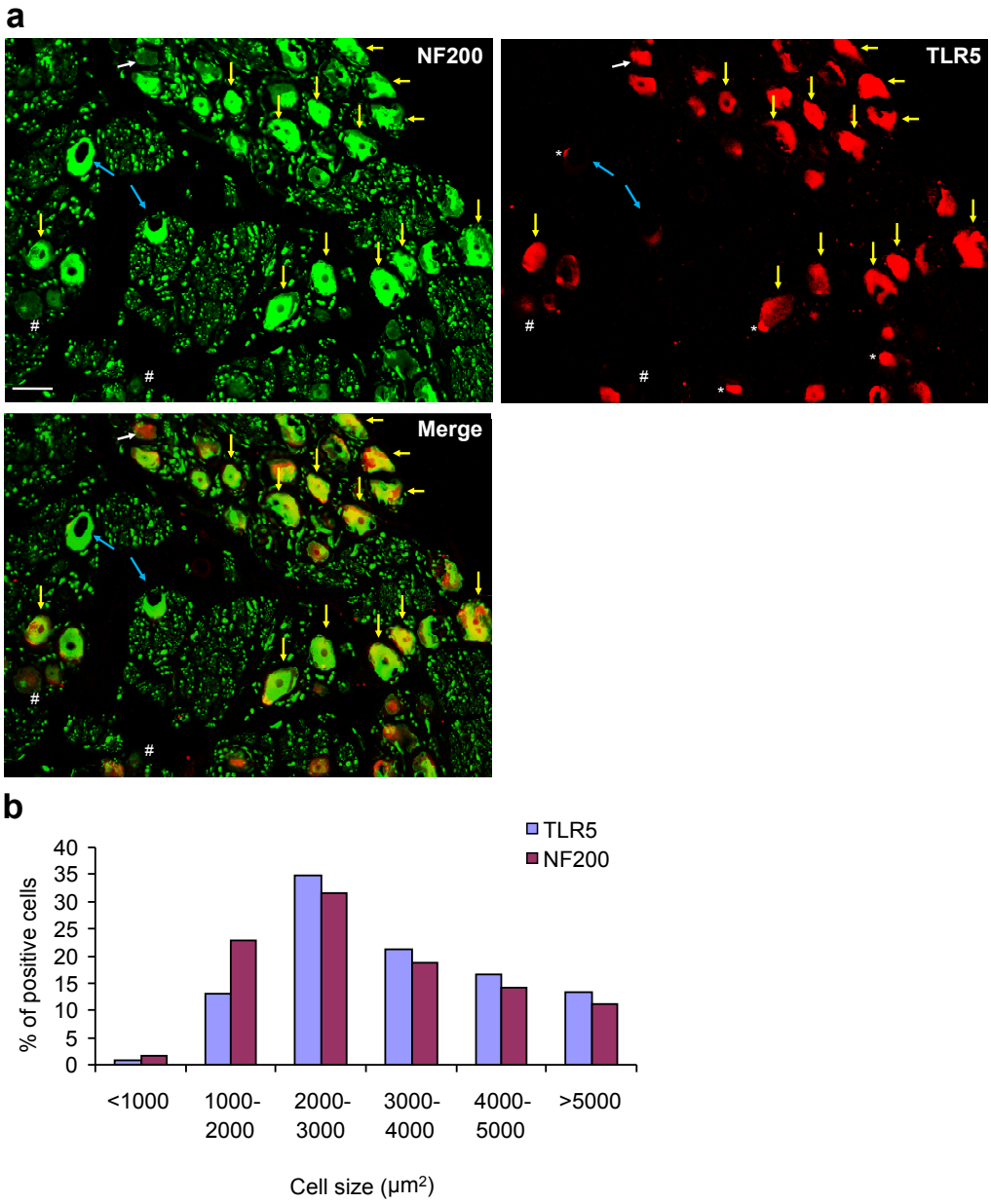

Supplementary Fig. 7. Co-localization of TLR5 with NF-200 in human DRG. (**a**) Double staining of TLR5 and NF200 in human L4 DRG section. Yellow, white, and blue arrows show double-labeled neurons, TLR5 single-labeled neurons, and NF200 single-labeled neurons, respectively. # denotes neurons that are TLR5- and NF200-negative. * indicates possible artifacts related to autofluorescence. Scale, 100 μm. (**b**) Size distribution of TLR5-IR and NF-200-IR neurons in human L4-L5 DRGs.

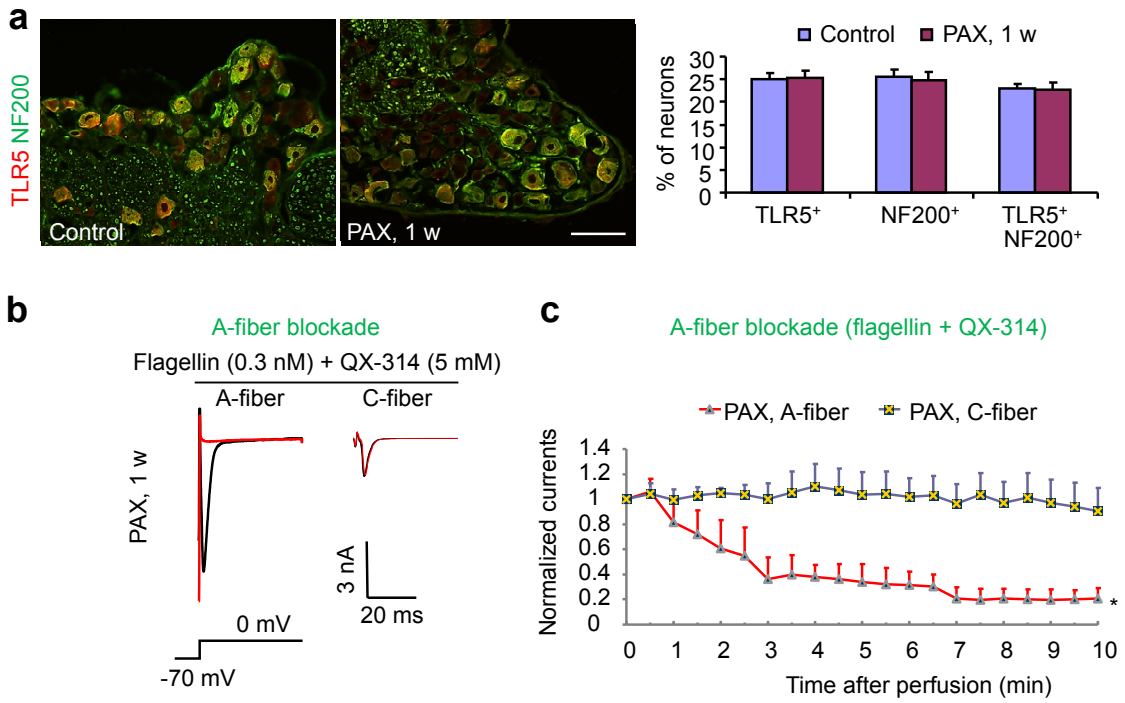

Supplementary Fig. 8. QX-314/flagellin treatment blocks A-fiber but not C-fiber activities in DRG neurons one week after paclitaxel (PAX) treatment. (**a**) Co-localization of TLR5 (red) and NF200 (green) in DRG sections of control mice and PAX-treated mice (1 w). Note that the percentage of DRG neurons expressing TLR5, NF200, and TLR5/NF200 is similar in control and PAX-treated mice. n = 4 mice / group. Scale, 100 μm. (**b**) Traces of transient sodium currents in C- and A-fiber neurons of WT mice, before and after the flagellin/QX-314 treatment. (**c**) Time course of sodium currents in C- (n = 5) and A-fiber (n = 8) neurons after the A-fiber blockade. *P < 0.05, two-way ANOVA. All data were expressed as mean ± s.e.m.

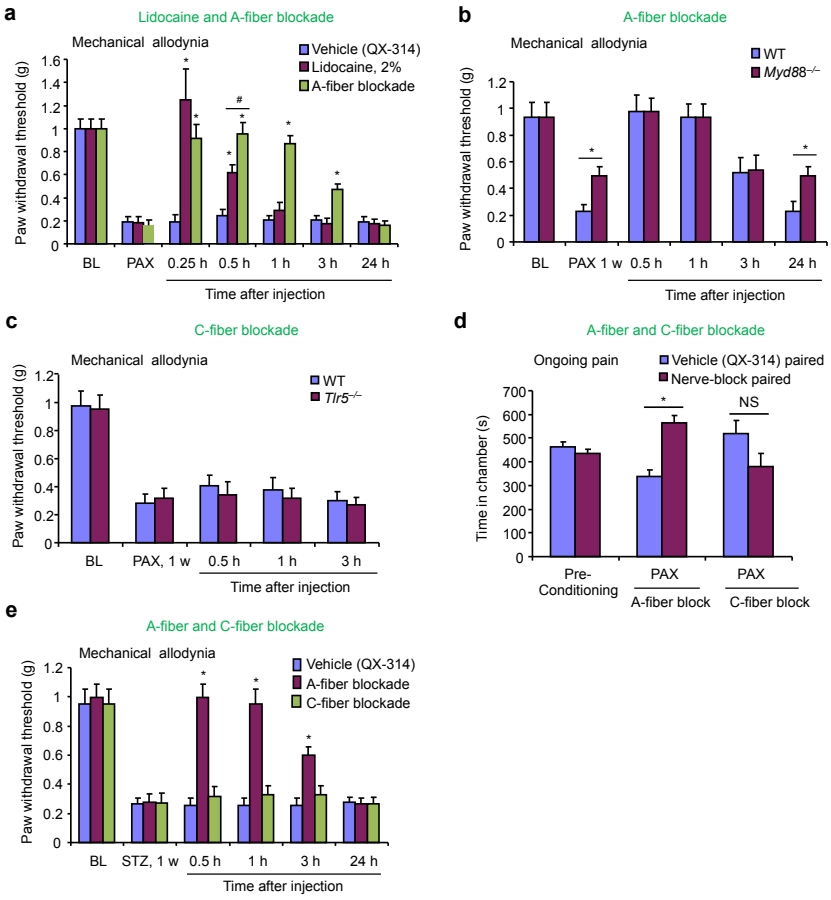

Supplementary Fig. 9. Effects of A-fiber blockade, C-fiber blockade, or lidocaine on paclitaxel (PAX)-induced mechanical allodynia and ongoing pain in WT, *Tlr5*$^{-/-}$, *Myd88*$^{-/-}$ mice. (**a**) Comparison of the effects of flagellin/QX-314 (A-fiber block) and 2% lidocaine on PAX-induced mechanical allodynia in WT mice. Note that lidocaine only produces a very transient reversal of allodynia (< 1 h). Behavior was tested 15 min after lidocaine treatment to avoid lidocaine-evoked motor impairment (<10 min). **P* < 0.05, vs. vehicle, $^{\#}P < 0.05$, two-way ANOVA followed by post-hoc Bonferroni test. *n* = 5 mice/group. (**b**) Reversal of PAX-induced mechanical allodynia by A-fiber blockade in *Myd88*$^{-/-}$ mice. PAX-induced mechanical allodynia is partially reduced after *Myd88* deletion. **P* < 0.05, vs. vehicle, two-way ANOVA followed by post-hoc Bonferroni test. *n* = 5 mice/group. (**c**) No effects of C-fiber blockade on PAX-induced mechanical allodynia in WT and *Tlr5*$^{-/-}$ mice. *n* = 5 mice/group. (**d**) CPP shows that mice spend more time in A-fiber blockade (*n* = 7 mice) paired chamber. Note C-fiber blockade (*n* = 5 mice) fails to show significant effects on CPP. **P* < 0.05, N.S, no significance. A-fiber and C-fiber blockade was induced by flagellin (0.3 μg) / QX-314 (0.2%) or capsaicin (10 μg) / QX-314 (0.2%), respectively, via intraplantar route. Lidocaine was also given via intraplantar injection. (**e**) Distinct effects of intraplantar A-fiber blockade vs. C-fiber blockade on STZ-induced mechanical allodynia. **P* < 0.05, two-way ANOVA followed by post-hoc Bonferroni test. *n* = 5 mice/group. All data were expressed as mean ± s.e.m.

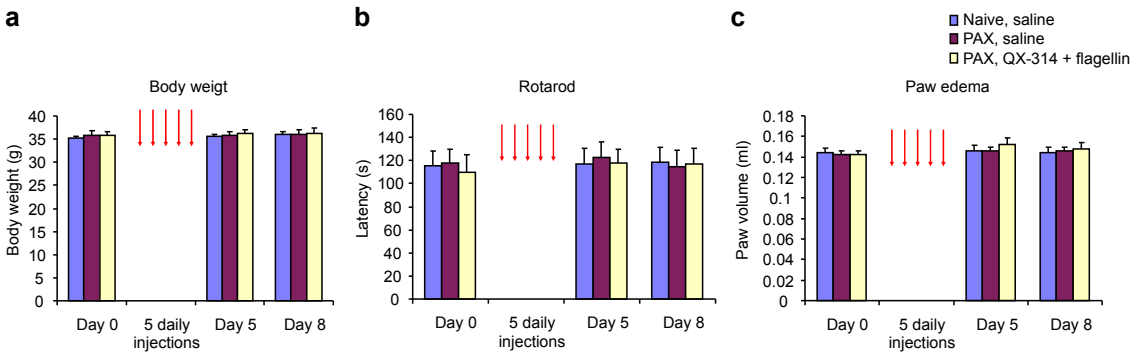

Supplementary Fig. 10. Effects of repeated intraplantar injections of flagellin (0.3 µg) and QX-314 (0.2%) on body weight, motor function (evaluated by Rotarod test), and paw inflammation (assessed by paw volume) in naïve and paclitaxel (PAX)-treated mice. n=5 mice/group. All data were expressed as mean ± s.e.m.

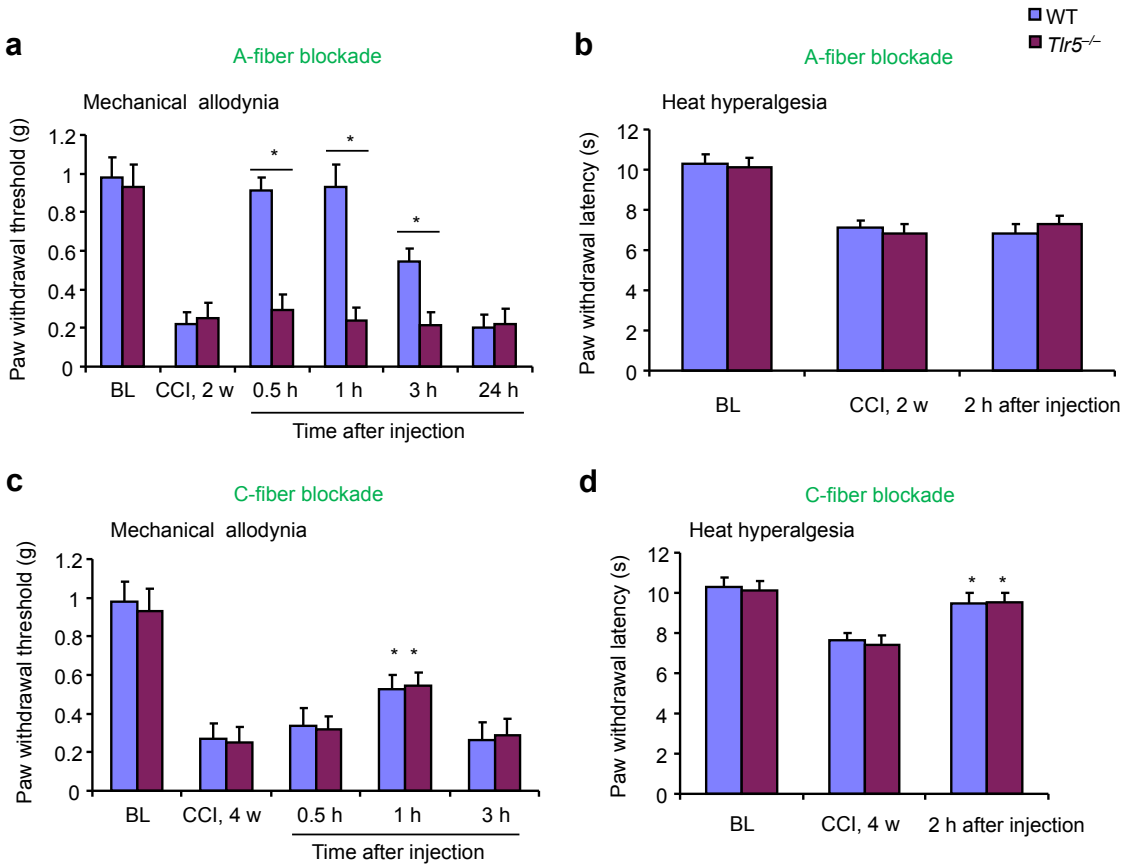

Supplementary Fig. 11. Distinct effects of A-fiber and C-fiber blockade on CCI-induced mechanical allodynia and heat hyperalgesia in WT and *Tlr5*$^{-/-}$ mice. (**a,b**) Reversal of CCI-induced mechanical allodynia (**a**) but not heat hyperalgesia (**b**) by A-fiber blockade in WT but not *Tlr5*$^{-/-}$ mice. **P* < 0.05, two-way ANOVA followed by post-hoc Bonferroni test. *n* = 5 mice/group. (**c,d**) Effects of C-fiber block on CCI-induced mechanical allodynia (**c**) and heat hyperalgesia (**d**) in WT and *Tlr5*$^{-/-}$ mice. Note that C-fiber block produces complete reversal of CCI-induced heat hyperalgesia but only mild reversal of CCI-induced mechanical allodynia and the blocking effect is *Tlr5*-independent. **P* < 0.05, two-way ANOVA followed by post-hoc Bonferroni test. *n* = 5 mice/group. A-fiber and C-fiber blockade was induced by flagellin (0.3 μg) / QX-314 (0.2%) or capsaicin (10 μg) / QX-314 (0.2%), respectively, via intraplantar route. All data were expressed as mean ± s.e.m.

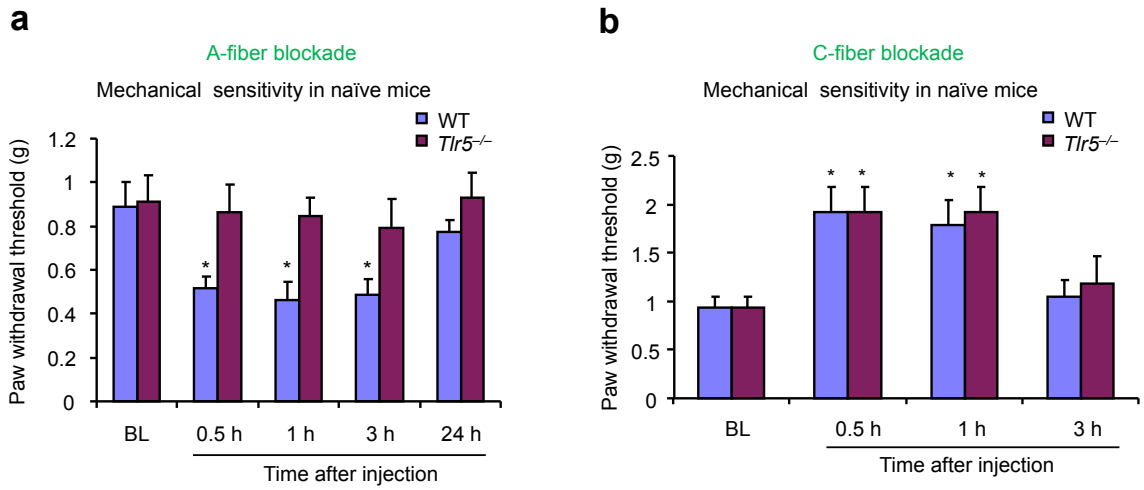

Supplementary Fig. 12. Different effects of intraplantar A-fiber blockade (**a**) and C-fiber blockade (**b**) on baseline mechanical sensitivity in naïve WT and *Tlr5*$^{-/-}$ mice. A-fiber blockade causes *Tlr5*-dependent mechanical hypersensitivity (allodynia). In contrast, C-fiber blockade causes *Tlr5*-independent mechanical hyposensitivity (analgesia) in naïve mice. A-fiber and C-fiber blockade was induced by flagellin (0.3 μg) / QX-314 (0.2%) or capsaicin (10 μg) / QX-314 (0.2%), respectively, via intraplantar route. **P* < 0.05, compared to baseline (BL), two-way ANOVA followed by post-hoc Bonferroni test. *n* = 5 mice/group. All data were expressed as mean ± s.e.m.